Published in final edited form as:
Bone. 2008 July ; 43(1): 25–31.

OXYGEN TENSION REGULATES PREOSTEOCYTE MATURATION AND MINERALIZATION

Adam Zahm, **Michael Bucaro**, **Vickram Srinivas**, **Irving M. Shapiro**, and **Christopher S. Adams**
Department of Orthopaedic Surgery, Thomas Jefferson University, Philadelphia, PA

Abstract

The goal of this investigation was to test the hypothesis that low pO_2 regulates bone cell mineralization. MLO-A5 and MLO-Y4 cells were cultured in monolayer and alginate scaffolds in hypoxia (2% O_2) or normoxia (20% O_2). Reduction of the O_2 tension from 20% to 2% resulted in reduced mineralization and decreased alkaline phosphatase activity of MLO-A5 cells in both monolayer and three-dimensional cultures. Similar changes in osteogenic activity were seen when these preosteocyte-like cells were subjected to chemical hypoxia. Likewise, in hypoxia, osteocyte-like MLO-Y4 cells exhibited reduced osteogenic activity when compared to normoxic controls. Based on these observations, it is concluded that a low pO_2 lowered the mineralization potential of bone cells at both early and late stages of maturation. Since the oxemic state is transduced by the transcription factor, HIF-1α, experiments were performed to determine if this protein was responsible for the observed changes in mineral formation. It was noted that when HIF-1α was silenced, mineralization activities were not restored. Indeed, in hypoxia, in relationship to wild type controls, the mineralization potential of the knockdown cells was further reduced. Based on these findings, it is concluded that the osteogenic activity of preosteocyte-like cells is dependent on both the O_2 tension and the expression of HIF-1α.

Keywords

Hypoxia; HIF; osteoblast; mineralization; μCT; MLO-A5; MLO-Y4

INTRODUCTION

In eukaryotic organisms, diatomic oxygen (O_2) is a ubiquitous regulator of cellular energetics and maturation. The high electronegative potential of O_2 is harnessed by cytochrome systems that drive cellular respiration [1]. This process is so efficient that organisms that can respire dominate the biosphere [2]. For almost all species, an absence of O_2 is incompatible with life, while a momentary lapse in O_2 delivery can result in impairment in cell function and frequently, promotes tissue destruction or organism death [3].

Not surprisingly, regulation of O_2 metabolism is carefully regulated. In almost all tissues, the molecular and cellular responses to a low O_2 tension is the activation of the transcription factor hypoxia-inducible factor 1 (HIF-1), a heterodimer composed of an O_2-sensitive α- and a

Communicating Author: Christopher S. Adams, Ph.D. Department of Orthopaedic Surgery Thomas Jefferson University Philadelphia, PA 19107 Email: Christopher.Adams@jefferson.edu Phone: 215-955-8754; Fax: 215-955-9159.

constitutively expressed β-subunit [4]. Stringent regulation of HIF-1, through O_2 sensitive sensor molecules, promotes the coordinated expression of a variety of target genes including those involved with angiogenesis, glycolysis and oxidative metabolism, cell proliferation, tissue remodeling, and erythropoiesis [5]. When expression of HIF-1 is disregulated or disturbed, there are gross disturbances in tissue function often leading to activation of a cell (apoptosis) or tissue death program [6,7,8,9,10].

Most tissues are well supplied with vascular elements that promote O_2 transport. However, in a number of tissues, especially those of the skeletal system, vessel density is low or non-existent. For example, in dentine, vessel density is very low, while the vascular supply to the epiphyseal growth plate is sparse, especially to those cells embedded in the cartilage core [6, 11]. In the latter case, HIF-1 directs the survival as well as differentiation of maturing chondrocytes [12]. In the Haversian system of compact bone, a heavily mineralized extracellular matrix impedes diffusion of O_2 from the central canal to the outlying osteocytes. Consistent with their expected low O_2 environment, osteocytes have previously been shown to express HIF-1 protein [13].

Unlike the osteocytes of cortical bone, osteoblasts are in close contact with marrow elements and the contiguous vasculature. In this environment, at O_2 tensions of 5–9%, osteoblasts exhibit well-formed and functional mitochondria [14] and, thus, can perform oxidative phosphorylation. At a lower pO_2, as cells become hypoxic or anoxic, there is inhibition of osteoblast phenotypic expression [15,16,17,18,19]. In a recent report, it was suggested that a low O_2 tension promotes the differentiation of osteoblasts into osteocytes [20]. The goal of the experiments described in this investigation is to assess the oxemic response of both mineralizing preosteocyte-like and osteocyte-like cells. Additionally, it is to determine if maturation and mineral deposition is dependent on the expression of HIF-1α. We report herein that in hypoxia, there is upregulation of HIF-1 and target genes, but inhibition of bone mineral formation.

MATERIALS AND METHODS

Bone cell culture

Murine long bone-derived osteocytic (MLO) A5 and Y4 cell lines, derived from transgenic mice expressing T-antigen driven by the osteocalcin promoter [21,22], were kindly provided by Dr. Lynda Bonewald (University of Missouri – Kansas City). The MLO-A5 cell line is representative of the mineralizing preosteocyte, whereas the MLO-Y4 cell line displays an osteocyte-like phenotype. Cells were cultured at 37°C, 5% CO_2, 95% air in α-MEM supplemented with 5% fetal bovine serum, 5% calf serum and antibiotics on tissue culture plastic dishes coated with rat tail collagen (BD Biosciences, San Jose, CA) as previously described [21,22]. In some cases, the culture media was supplemented with 10 mM β-glycerophosphate (Sigma-Aldrich, St. Louis, MO). For studies of adherent cell mineralization, cells were plated at a density of $1.0–1.5 \times 10^4/cm^2$; for measurement of alkaline phosphatase activity, cells were plated at a density of $5–7\times10^4$ (for 24 h measurements) or $7.5\times10^3/cm^2$ for extended periods (7–8 days). Hypoxic experiments were performed at 2% or 5% O_2 in the in$VIVO_2$ Hypoxia Workstation (Rushkinn, Cincinnati, OH). To stabilize HIF-1α at 20% O_2, the culture medium was supplemented with 130 μM desferrioxamine mesylate (Sigma-Aldrich, St. Louis, MO) [23].

Encapsulation of osteoblast-like cells in alginate

MLO-Y4 and MLO-A5 cells were released from monolayer culture by trypsinization, resuspended in media and mixed 1:1 (v/v) with 2 % ultrapure medium-viscosity alginate in isotonic NaCl (NovaMatrix-FMC BioPolymer, Philadelphia, PA) to obtain a final

concentration of 2.5×10^6 cells/mL in 1% alginate [24]. The alginate/cell mixture was transferred to a 5 mL syringe, mounted in a syringe pump (Harvard Apparatus, Holliston, MA). The alginate encapsulated cells were extruded from the syringe through an 18½ gauge needle at a rate of 50 mL/h into a continuously stirred cross linking bath (75 mM NaCl, 50 mM $CaCl_2$) [24]. The alginate formed spherical beads approximately 2.75 mm in diameter. After 10 min. the beads were transferred to 6 well culture dishes containing 5 mL culture medium. For computer microtomography (μCT) (Scanco, King of Prussia, PA) analysis, the beads were maintained in culture media with 10 mM β-glycerophosphate supplemented with 1 mM $CaCl_2$.

Alkaline phosphatase activity and staining of adherent and encapsulated cells

Cells were washed twice in PBS and lysed with 200 μL 0.5% TritonX-100. Plates were then frozen at −80°C, thawed, and centrifuged for 3 min at 12,000 rpm at 4°C. 50 μL of supernatant was transferred to a 96 well plate and 150 μL of SIGMA*FAST*™ p-nitrophenyl phosphate solution (Sigma-Aldrich, St. Louis, MO) was added to each well. Absorbance at 430 nm was measured in a Tecan plate reader at 0 and 30 min. Total protein was determined using a BCA Protein Assay Kit (Pierce, Rockford, IL) and alkaline phosphatase activity was calculated as ng p-nitrophenol/min/μg protein. For studies of encapsulated osteoblasts, beads were solubilized in 25 mM sodium citrate, 10 mM EDTA, 115 mM NaCl, pH 7.4 for 15 min at 37° C. Cells were pelleted by centrifugation and then lysed in 200 μL 0.5% TritonX-100, frozen at -80°C and immediately thawed, centrifuged, and alkaline phosphatase activity was determined as described above. For staining, cells were incubated with 1 mM naphthol As-Bi phosphate (Sigma-Aldrich, St. Louis, MO) and 3.9 mM Fast Red TR Salt (Sigma-Aldrich, St. Louis, MO) in 50 mM Tris-HCl for 20 min at 37°C. Following incubation, cells were fixed in 3.7% formaldehyde for 15 min. The stained samples were viewed microscopically and images of the stained wells obtained digitally.

Assessment of osteoblast-like cell mineralization

Mineralization was assessed by using the Von Kossa technique and digital image analysis. To quantitatively measure mineralization, the formaldehyde-fixed cells were treated with 2% Alizarin Red S (Sigma-Aldrich, St. Louis, MO) for 5 min and washed in distilled H_2O. Measurement of Alizarin Red staining was performed as described by Wang et al. [25]. Briefly, bound alizarin red was dissolved in 1 mL of 100 mM cetylpyridinium chloride and absorbance at 590 nm was measured using a Tecan plate reader. Values were corrected for total protein isolated from replicate wells. Mineral produced by MLO-A5 cells encapsulated in alginate beads was assessed by μCT. Single alginate beads were placed in a scanning tube of 12.3 mm diameter, and scanned at a voxel resolution of 12 μm^3 with energy and intensity settings of 45,000 V and 177 μA and segmentation values of 0.8/1/153 for Day 7 and 0.8/1/204 for Day 14 measurements. Mineralization values are reported as total mineralized volume (MV).

Quantification of Live/Dead cells

Quantification of living and dead cells in the alginate beads was performed as described previously [24]. The beads were treated with 10 μM Cell Tracker™ Green CMFDA (Invitrogen, Carlsbad, CA) and 10 μg/mL propidium iodide in phenol red-free Hank's Balanced Salt Solution for 5 min. The beads were imaged by confocal microscopy (Olympus Fluoview, Center Valley, PA). Optical image stacks were collected at 10 μm steps to a depth of 100 μm, and rendered as an overlay.

Expression of osteogenic genes by RT-PCR

Cells were scraped from 100 mm dishes in ice cold PBS and collected by centrifugation. RNA was isolated from cell pellets using an RNeasy® Protect Mini Kit (Qiagen, Valencia, CA)

according to the manufacturer's protocol and was stored at −80°C. RNA yield was determined spectrophotometrically. Each reaction contained 22 ng RNA and 0.4 μM of primer. The RNA was reverse transcribed and then amplified using Superscript One-Step RT-PCR Kit with Ready-To-Go™ RT-PCR Beads (GE Healthcare Bio-Sciences, Piscataway, NJ). Band signal quantification was performed using NIH ImageJ software. The primers are listed in Table 1.

Western blot analysis of HIF-1α expression in osteoblast-like cells

Cells were collected in lysis buffer (150 mM NaCl, 1 mM DTT, 500 μM NaF, 500 μM Na_3VO_4, Complete Protease Inhibitors in MPER) and kept on ice for 45 min, centrifuged at 10,000 rpm for 10 min at 4°C and the supernatant stored at −80°C. Protein concentration was determined using a BCA Protein Assay Kit (Pierce, Rockford, IL). 100 μg of sample protein was diluted 1:2 in Laemeli Sample Buffer (Bio-Rad, Hercules, CA) and heated at 100° C for 5 min. Samples were then electrophoresed in 1X TGS buffer (25 mM Tris, 192 mM glycine, 0.1% (w/v) SDS, pH 8.3), transferred onto a Immobilon™ –P Transfer Membrane (Millipore, Billerica, MA) in 1X Tris/Glycine Buffer (25 mM Tris, 192 mM glycine, 20% (v/v) methanol, pH 8.3. Membranes were blocked in blocking buffer (5% instant nonfat dry milk in 1X TBS) for 30 min and then incubated with primary antibodies for 3 h at room temperature: mouse anti-HIF-1α, (R&D Systems, Minneapolis, MN) and goat anti-β-actin, (Santa Cruz Biotechnology, Santa Cruz, CA). The antibodies were diluted 1:1000 in blocking buffer. Membranes were then washed in 1X TBS and incubated with secondary antibodies (Goat anti-mouse AP conjugate, SouthernBiotech, Birmingham, AL; Donkey anti-goat IgG AP conjugate, Promega, Madison, WI) diluted 1:1000 in blocking buffer for 45 min at room temperature. Membranes were washed twice in 1X TBS and incubated with Western Blue® Stabilized Substrate for Alkaline Phosphatase (Promega, Madison, WI). Protein bands were imaged using a Epson Expression 1600 scanner. Band signal quantification was performed using NIH ImageJ software.

Suppression of HIF-1α using siRNA technology

A siRNA combination kit (Promega, Madison, WI) was utilized to downregulate HIF-1α. The following phosphorylated forward (f) and reverse (r) oligonucleotides were used: f – 5′ GTCCAGAGTCACTGGGACT 3′; r – 5′TCAGGGTCACTGAGACCTG 3′ (corresponding to nucleotides 1438–1457 of the mouse HIF-1α mRNA). Permanent cell lines were generated using 80% confluent monolayers transfected with the siRNA vector. Clonal selection was performed using 2μg/mL puromycin. A cell line with the reversed sequence was used as a control. Changes in expression levels were verified by both RT-PCR and Western blot analysis.

Statistical Analysis

Statistical analysis was performed using SigmaStat 2.03 (Systat; Richmond, CA) software. Normal data with equal variance was analyzed using a one-way ANOVA test with a Tukey post hoc procedure. A Kruskal-Wallis ANOVA on ranks with a Dunns post hoc test was used where the data sets were not normal. Significance was assessed when $p < 0.05$. Values in each graph represent mean and SEM. Alkaline phosphatase assays were performed at least three times, with representative data presented; all other assays (Von Kossa and alizarin staining, Live/Dead staining, and μCT, Western and PCR analyses) were performed at least twice.

RESULTS

Alkaline phosphatase activity and mineralization is reduced at low pO_2

To test the hypothesis that bone cell maturation is regulated by pO_2, MLO-A5 and MLO-Y4 cells were cultured at 2% or 20% O_2. At 2% O_2, on day 9, both cell types exhibit reduced alkaline phosphatase (AP) staining (Fig. 1A). A similar, more dramatic change is evident when

the enzyme activity was determined (Fig. 1B). Both MLO-A5 and MLO-Y4 cells display significantly reduced alkaline phosphatase activity after 7 days of culture at 2% O_2 compared to 20% O_2. A reduction in pO_2 elicits a dose-dependent decrease in MLO-A5 alkaline phosphatase activity (Fig. 1C).

We next examined mineralization of MLO cells in the presence of β-glycerophosphate at 2% or 20% O_2 after 9 days of culture. At 20% O_2, MLO-A5 cells display positive Von Kossa staining. The staining is greatly decreased at 2% O_2 (Fig. 1D). Measurement of the change in mineral deposition is even more dramatic when evaluated by Alizarin Red S. Figure 1E shows that after 7 days of culture there is a 7 fold decrease in staining at 2% O_2. In contrast to MLO-A5 cells, the MLO-Y4 cells show minimal Von Kossa staining at both O_2 tensions (Fig 1D).

Preosteocyte-like cells, in three-dimensional culture, exhibit reduced alkaline phosphatase activity and matrix mineralization at a low pO_2

To further explore the effect of the oxemic state on preosteocyte maturation, MLO-A5 cells were encapsulated in alginate beads. After 7 days of culture in 2% O_2, MLO-A5 cells in alginate beads exhibit a considerable decrease in alkaline phosphatase staining (Fig. 2A), and a 5-fold decrease in alkaline phosphatase activity (Fig. 2B). To confirm that changes in alkaline phosphatase activity in alginate were not due to a decrease in cell viability at 2% O_2, cells were treated with Cell Tracker™ Green (Invitrogen, Carlsbad, CA) and propidium iodide (Fig. 2C). Figure 2D shows that there is no significant difference in the live\dead ratios in the 2% and 20% cultures. Thus, a lowered pO_2 does not trigger a change in cell number.

Mineral formation by MLO-A5 cells in alginate beads is visually evident by day 5 (Fig. 3A). The mineral produced in these three-dimensional cultures was quantified by μCT. At 7 days, at 20% O_2, mineral formation is largely pericellular as indicated by the small, approximately cell-sized loci of mineralization. At 2% O_2, there is a considerable reduction in the number of pericellularly mineralized deposits (Fig 3B). At 14 days, the mineral in the alginate beads cultured at 20% O_2 is presented, in the thresholded image, as a solid sphere. A cross-sectional image of the bead reveals that the majority of the mineral is restricted to the periphery (Fig. 3C). When the total mineralized volume (TMV) of the beads cultured at the two O_2 tensions are compared, it is clear that the mineral volume is greatly increased at 20% O_2 at both 7 and 14 days (Table 2). In addition, the mineralized surface area to volume ratio (BS/BV) is significantly lower in beads cultured at 20% O_2, indicating the formation of larger mineral aggregates (Table 2).

Reduced pO_2 stabilizes HIF-1α protein and induces expression of HIF-1α target genes

We evaluated expression of the transcription factor, HIF-1α, in MLO cells at 2% O_2. Western blot analysis indicates that the hypoxic response in MLO-A5 cells is characterized by an increase in HIF-1α expression (Fig. 4A). We next examined the expression of HIF-1α target genes in MLO-A5 cells cultured at 2% O_2. In hypoxia, expression of the HIF-1α target genes, GLUT-1 and Bnip-3, is upregulated 3-fold by 12 h (Fig. 4B). The expression of RUNX-2, the critical bone-specific transcription factor, is only slightly influenced by pO_2 (Fig. 4C). In contrast, osterix expression is reduced 50% in 12h.

Chemical hypoxia stabilizes HIF-1α protein, induces expression of HIF-1α targets, and inhibits alkaline phosphatase activity

To differentiate between an increase in HIF-1α and other effects of a low O_2 environment, we blocked HIF-1α degradation at 20% O_2 using desferrioxamine. Desferrioxamine treatment of both MLO-A5 and MLO-Y4 cells for 24 h in 20% O_2 upregulates HIF-1α protein levels and HIF-1α target gene (Bnip-3 and GLUT-1) expression to levels similar to those seen in hypoxia (Fig. 5A and B). In addition, alkaline phosphatase activity is significantly reduced in MLO-

A5 cells treated with desferrioxamine at 20% O_2 (Fig. 5C). The results of desferrioxamine treatment of MLO-Y4 cells are similar to those noted for MLO-A5 preosteocyte-like cells (Fig. 5C).

Silencing of HIF-1α in preosteocyte-like cells further reduces alkaline phosphatase activity and mineralization

To determine whether HIF-1α is responsible for the inhibition of MLO-A5 alkaline phosphatase activity and mineralization, we suppressed HIF-1α protein levels using siRNA technology (Fig. 6A). The marked decrease in HIF-1α protein levels, as well as a low level of expression of the HIF-1α target, Bnip-3, at 2% O_2 is indicate of effective suppression (Fig. 6B). When normalized to the alkaline phosphatase activity at 20% O_2, enzyme activity is significantly reduced in the silenced cells at 2% O_2 (Fig. 6C). In addition, alizarin red staining of the HIF-1α knockdown cells is very low at this pO_2 (Fig. 6D). Note that, while the control cells still exhibit some alizarin red positive staining at 2%, the HIF-1α silenced cells display minimal staining. This decrease in the capacity of the silenced cells to form mineral is evident at both 2% and 20% O_2. These results suggest that the decrease in mineralization, evident in the low O_2 environment, is either independent of, or inhibited by HIF-1α.

DISCUSSION

The goal of this investigation was to test the hypothesis that the environmental pO_2 influences osteogenic function. We demonstrated that a low oxemic environment degraded activities linked to formation of a calcified extracellular matrix. Reduction of the O_2 tension from 20% to 2% resulted in reduced mineralization and decreased alkaline phosphatase activity of MLO-A5 cells in both monolayer and three-dimensional cultures. Similar changes in osteogenic activity were seen when these preosteocyte-like cells were subjected to chemical hypoxia. Likewise, in hypoxia, osteocyte-like MLO-Y4 cells exhibited reduced osteogenic activity when compared to normoxic controls. Based on these observations, it is concluded that a low pO_2 lowered the mineralization potential of bone cells at both early and late stages of maturation. Since the oxemic state is transduced by the transcription factor, HIF-1α, experiments were performed to determine if this protein was responsible for the observed changes in mineral formation. It was noted that when HIF-1α was silenced, mineralization activities were not restored. Indeed, in hypoxia, in relationship to wild type controls, the mineralization potential of the knockdown cells was further reduced. Based on these findings, it is concluded that the osteogenic activity of preosteocyte-like cells is dependent on both the O_2 tension and the expression of HIF-1α.

In bone, as well as cartilage, cells adapt to a low pO_2 by upregulating the activity of one or more sensor proteins, prolyl hydroxylases [12]; these sensors trigger the transcription of members of the HIF family of proteins. We hypothesized that in bone, stabilization of HIF-1α mediated the reduction in the mineralization potential of differentiating osteocytes. Indeed, previous studies have demonstrated that hypoxia regulated HIF-1α expression in osteocytes in vivo [26,13]. As expected, we found that HIF-1α was induced in preosteocyte-like cells by both a low pO_2, as well as chemical hypoxia. In addition, there was coordinate up-regulation of the HIF-1α target genes, Bnip-3 and GLUT-1. These results were consistent with the hypothesis that HIF-1α regulated the mineralization response of preosteocyte-like cells to hypoxic conditions. To confirm that this oxemic response was mediated by HIF-1α, we silenced the gene using siRNA technology. The siHIF-1α cells exhibited a reduction in alkaline phosphatase activity and a loss of mineral formation in normoxia. When these cells were exposed to low pO_2, a further loss of mineralization potential was observed, suggesting that the decreased mineralization potential of the MLO-A5 cells was not dependent on the activity of HIF-1α. Furthermore, since there was a loss of alkaline phosphatase activity in the

silenced cells even in normoxia, HIF-1α may serve to activate one or more events that are required for bone formation. Of course, it remains possible that the downregulation of mineralization in hypoxia is regulated by other members of the HIF family or other sensor proteins. Nevertheless, based on the results of the current study, it is concluded that, as a response to the reduction in O_2 availability, HIF-1α may transduce signals that are concerned with the promotion of one or more mineralization-related activities.

One explanation for the reduction in mineral formation by MLO-A5, cells cultured at a low O_2 tension, is that in response to hypoxia, the cells dedifferentiate. However, the observation that there was little change in the expression of RUNX2 and osterix along with the maintenance of the dendritic cell shape at a low pO_2 suggests that the differentiation state is maintained. Moreover, a recent report has shown only a minimal change in RUNX2 mRNA expression in mouse calvarial osteoblasts at 2% O_2 [19]. In fact, Hirao et al. reported that maturation of MC3T3-E1 preosteoblasts, as well as osteoblasts and osteocytes in calvarial organ culture was accelerated when cultured at low 5% pO_2 [20]. It was noted that matrix mineralization was enhanced, while alkaline phosphatase activity was decreased in hypoxic cell and organ cultures. Other workers have confirmed that hypoxia causes a significant reduction in alkaline phosphatase activity [15,27,17]. Therefore, the observation that bone cells maintained their osteogenic potential in a hypoxic environment is well supported by previously reported work and provided further evidence that, during differentiation, osteoblasts accommodate to matrix-dependent gradients in O_2 tension.

A shortcoming of conventional monolayer cultures for the study of bone formation *in vitro* is the restriction of cell growth to two dimensions. For this reason, we encapsulated preosteocytes in alginate and again evaluated the effect of O_2 tension on mineralization. Alginate provides a scaffold that mimics the three-dimensional nature of the *in vivo* tissue. The alginate beads also permitted quantification of mineral deposition by μCT analysis. Confirming the results of our monolayer culture studies at 2% O_2, we observed reductions in both alkaline phosphatase activity and mineralization. Since the μCT analysis provided a three dimensional image of the cultures system, it was evident that cell-mediated mineral deposition was highest at the bead periphery. One explanation for this observation is that a gradient in environmental conditions exist in the bead that influence cell function. With respect to O_2, due to its utilization by cells of the periphery of the bead and limitations on the rate of diffusion from the medium to the bead center, depletion in the bead interior might be expected. As discussed below, a similar type of O_2 gradient would be expected to occur in bone in vivo. This result suggests that mineralization is optimal at a specific pO_2, an observation which further supports our hypothesis that the pO_2 is a critical signal controlling the mineralization potential of bone cells.

One critical implication of the findings discussed above is that there must exist a basal threshold of tissue oxygenation that supports the ordered regulation of mineral in the extracellular matrix by osteoid-producing and mineralization-directing osteoblasts. Accordingly, those cells that are engulfed in matrix and at a distance from the marrow surface (maturing preosteocytes), would be expected to exist at a pO_2 lower than that experienced by the more superficial bone cells. For cells subsumed within the mineralized tissue matrix, there would be reliance on glycolysis, depression of anabolic function, and loss of ability to express alkaline phosphatase, an enzyme required for biological mineralization [29]. Cells adherent to the bone surface would have the same or slightly lower O_2 concentration as the surrounding vascular channels, a value recorded as approximately 5–9% [28]. The presence of these actively respiring oxygen-dependent osteoblasts, together with the accumulating layers of osteoid and mineralized osteoid, would serve to generate an O_2 diffusion gradient. From this perspective, it would follow that there is a basal threshold of tissue oxygenation that facilitates the regulated deposition of mineral in the extracellular matrix by osteoid-producing and mineralization-directed osteoblasts. Moreover, this observation may explain why osteocytes, buried in

mineralized bone, and at a lower pO_2 than the more superficial osteoblasts display a low alkaline phosphatase activity and minimal mineralization potential in vivo [30].

From a disease perspective, decriments in O_2 delivery, such as those mediated by ischemia, anemia or atherosclerosis would profoundly impact new bone formation. While explanations for many of these conditions have focused primarily on impairment of resorptive activity, the results of this study suggest that limitations in O_2 supply may very well affect the formative components of the remodeling process. Experiments are in progress to map the oxygen gradients within both normal and diseased bone and to define those tensions that maximally support osteoblast/osteocyte function.

Acknowledgements

Supported in part by NIH grants DE-10875, DE-016383, AR-052273 and by a grant from the Commonwealth of Pennsylvania,

References

1. Semenza GL. Life with Oxygen. Science 2007;318(5847):62–64. [PubMed: 17916722]
2. Lane, N. Oxygen: The molecule that made the world. Oxford: Oxford University Press; 2002.
3. Kulkarni AC, Kuppusamy P, Parinandi N. Oxygen, the lead actor in the pathophysiologic drama: Enactment of the trinity of normoxia, hypoxia, and hyperoxia in disease and therapy. Antioxidants & Redox Signaling 2007;9(10):1717–1730. [PubMed: 17822371]
4. Wenger RH, Gassmann M. Oxygen(es) and the hypoxia-inducible factor-1. Biological Chemistry 1997;378(7):609–616. [PubMed: 9278140]
5. Wenger RH. Cellular adaptation to hypoxia: O2-sensing protein hydroxylases, hypoxia-inducible transcription factors, and O2-regulated gene expression. FASEB Journal 2002;16(10):1151–1162. [PubMed: 12153983]
6. Schipani E, Ryan HE, Didrickson S, Kobayashi T, Knight M, Johnson RS. Hypoxia in cartilage: HIF-1alpha is essential for chondrocyte growth arrest and survival. Genes & Development 2001;15 (21):2865–2876. [PubMed: 11691837]
7. Biju MP, Neumann AK, Bensinger SJ, Johnson RS, Turka LA, Haase VH. Vhlh gene deletion induces Hif-1-mediated cell death in thymocytes. Molecular & Cellular Biology 2004;24(20):9038–9047. [PubMed: 15456877]
8. Zhang Q, Zhang ZF, Rao JY, Sato JD, Brown J, Messadi DV, Le AD. Treatment with siRNA and antisense oligonucleotides targeted to HIF-1alpha induced apoptosis in human tongue squamous cell carcinomas. International Journal of Cancer 2004;111(6):849–857.
9. Huang Y, Hickey RP, Yeh JL, Liu D, Dadak A, Young LH, Johnson RS, Giordano FJ. Cardiac myocyte-specific HIF-1alpha deletion alters vascularization, energy availability, calcium flux, and contractility in the normoxic heart. FASEB Journal 2004;18(10):1138–1140. [PubMed: 15132980]
10. Tomita S, Ueno M, Sakamoto M, Kitahama Y, Ueki M, Maekawa N, Sakamoto H, Gassmann M, Kageyama R, Ueda N, Gonzalez FJ, Takahama Y. Defective brain development in mice lacking the Hif-1alpha gene in neural cells. Molecular & Cellular Biology 2003;23(19):6739–6749. [PubMed: 12972594]
11. Shapiro IM, Mansfield KD, Evans SM, Lord EM, Koch CJ. Chondrocytes in the endochondral cartilage are not hypoxic. American Journal of Physiology 1997;272:C1134–C1143. [PubMed: 9142837]
12. Terkhorn SP, Bohensky J, Shapiro IM, Koyama E, Srinivas V. Expression of HIF prolyl hydroxylase isozymes in growth plate chondrocytes: Relationship between maturation and apoptotic sensitivity. Journal of Cellular Physiology 2007;210(1):257–265. [PubMed: 17044072]
13. Gross TS, Akeno N, Clemens TL, Komarova S, Srinivasan S, Weimer DA, Mayorov S. Selected Contribution: Osteocytes upregulate HIF-1alpha in response to acute disuse and oxygen deprivation. Journal of Applied Physiology 2001;90(6):2514–2519. [PubMed: 11356821]
14. Gay C, Schraer H. Frozen thin-sections of rapidly forming bone: bone cell ultrastructure. Calcified Tissue Research 1975;19(1):39–49. [PubMed: 1201464]

15. Matsuda N, Morita N, Matsuda K, Watanabe M. Proliferation and differentiation of human osteoblastic cells associated with differential activation of MAP kinases in response to epidermal growth factor, hypoxia, and mechanical stress in vitro. Biochemical & Biophysical Research Communications 1998;249(2):350–354. [PubMed: 9712699]

16. Utting JC, Robins SP, Brandao-Burch A, Orriss IR, Behar J, Arnett TR. Hypoxia inhibits the growth, differentiation and bone-forming capacity of rat osteoblasts. Experimental Cell Research 2006;312 (10):1693–1702. [PubMed: 16529738]

17. Park JH, Park BH, Kim HK, Park TS, Baek HS. Hypoxia decreases Runx2/Cbfa1 expression in human osteoblast-like cells. Molecular & Cellular Endocrinology 2002;192(1–2):197–203. [PubMed: 12088880]

18. D'Ippolito G, Diabira S, Howard GA, Roos BA, Schiller PC. Low oxygen tension inhibits osteogenic differentiation and enhances stemness of human MIAMI cells. Bone 2006;39(3):513–522. [PubMed: 16616713]

19. Salim A, Nacamuli RP, Morgan EF, Giaccia AJ, Longaker MT. Transient changes in oxygen tension inhibit osteogenic differentiation and Runx2 expression in osteoblasts. J Biol Chem 2004;279(38): 40007–40016. [PubMed: 15263007]

20. Hirao M, Hashimoto J, Yamasaki N, Ando W, Tsuboi H, Myoui A, Yoshikawa H. Oxygen tension is an important mediator of the transformation of osteoblasts to osteocytes. Journal of Bone and Mineral Metabolism 2007;25(5):266–276. [PubMed: 17704991]

21. Kato Y, Windle JJ, Koop BA, Mundy GR, Bonewald LF. Establishment of an osteocyte-like cell line, MLO-Y4. Journal of Bone & Mineral Research 1997;12(12):2014–2023. [PubMed: 9421234]

22. Kato Y, Boskey A, Spevak L, Dallas M, Hori M, Bonewald LF. Establishment of an osteoid preosteocyte-like cell MLO-A5 that spontaneously mineralizes in culture. Journal of Bone & Mineral Research 2001;16(9):1622–1633. [PubMed: 11547831]

23. Wang GL, Semenza GL. Desferrioxamine induces erythropoietin gene expression and hypoxia-inducible factor 1 DNA-binding activity: implications for models of hypoxia signal transduction. Blood 1993;82(12):3610–3615. [PubMed: 8260699]

24. Bucaro M, Zahm AM, Risbud MV, Ayyaswamy P, Mukundakrishnan K, Steinbeck M, Shapiro IM, Adams CS. The effect of simulated microgravity on osteoblasts is independent of the induction of apoptosis. Journal of Cellular Biochemistry. 2007In Press

25. Wang W, Xu J, Du B, Kirsch T. Role of the progressive ankylosis gene (ank) in cartilage mineralization. Molecular & Cellular Biology 2005;25(1):312–323. [PubMed: 15601852]

26. Dodd JS, Raleigh JA, Gross TS. Osteocyte hypoxia: a novel mechanotransduction pathway. American Journal of Physiology 1999;277(3 Pt 1):C598–C602. [PubMed: 10484347]

27. Kubota M. Study on proliferation and function of periodontal ligament fibroblasts and osteoblastic cells under hypoxia. Kokubyo Gakkai Zasshi 1989;56(4):473–484. [PubMed: 2621392]

28. Ishikawa Y, Ito T. Kinetics of hemopoietic stem cells in a hypoxic culture. European Journal of Haematology 1988;40(2):126–129. [PubMed: 3278928]

29. Murshed M, Harmey D, Millan JL, McKee MD, Karsenty G. Unique coexpression in osteoblasts of broadly expressed genes accounts for the spatial restriction of ECM mineralization to bone. Genes Dev 2005;19(9):1093–1104. [PubMed: 15833911]

30. Doty, SB.; Schofield, BH. Histochemistry and enzymology of bone forming cells. In: Hall, BK., editor. Bone Vol 1: The Osteoblast and Osteocyte. 1990. p. 71-102.

31. Parfitt AM, Mathews CH, Villanueva AR, Kleerekoper M, Frame B, Rao DS. Relationships between surface, volume, and thickness of iliac trabecular bone in aging and in osteoporosis. Implications for the microanatomic and cellular mechanisms of bone loss J Clin Invest 1983;72(4):1396–1409.

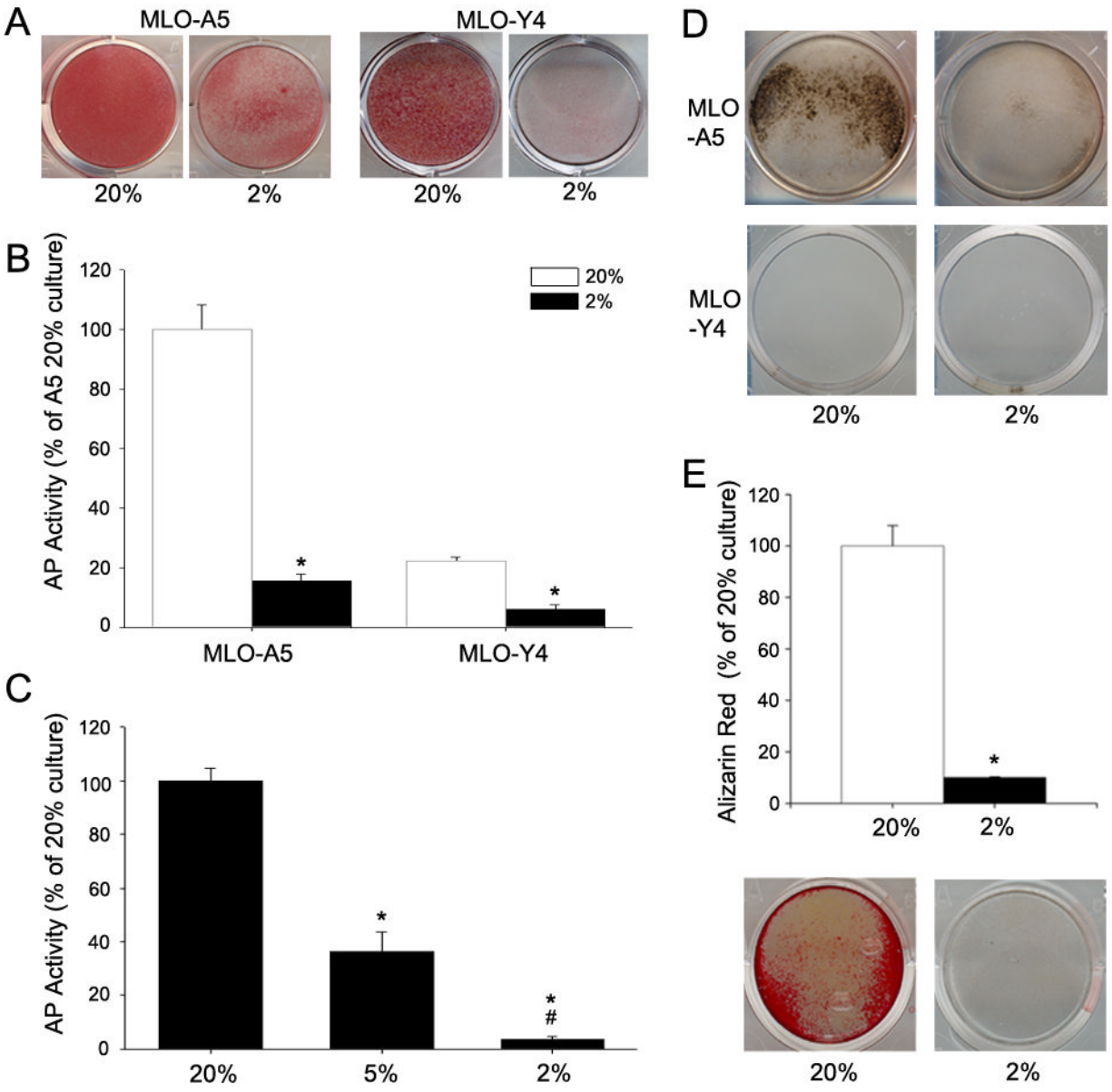

Figure 1.

Alkaline phosphatase (AP) activity and mineralization status of MLO cells as a function of O_2 tension. (A) AP stained MLO-A5 and MLO-Y4 cells after 9 days of culture at 20% or 2% O_2. Both cell lines showed markedly lower staining at 2% O_2. (B) AP activity of MLO-A5 and MLO-Y4 cells after culture for 7 days at 20 or 2% O_2. AP activity was lower in both cell lines at 2% compared to 20% O_2. Data is shown is expressed as ng/min/μg protein and normalized to 20% O_2 values for each cell type. (C) AP activity of MLO-A5 cells after 7 days culture at 2, 5, and 20% O_2. Note as the pO2 was reduced, there was a corresponding decrease in AP activity. (D) Von Kossa stained MLO cells after 9 days in culture at 20 and 2% O_2. Staining is negative for MLO-Y4 cells and positive for MLO-A5 cells at both 2% and 20% O_2; there is robust staining of the cultures at 20% O_2 (E) Alizarin Red stained MLO-A5 cells after 7 days in culture at 20% or 2% O_2. Staining was 7-fold higher at 20% O_2 than at 2% O_2. Bottom panel shows representative wells stained with Alizarin Red. Values plotted are mean and SEM. * significantly different from 20% O_2; # significantly different from 5% O_2; $p<0.05$.

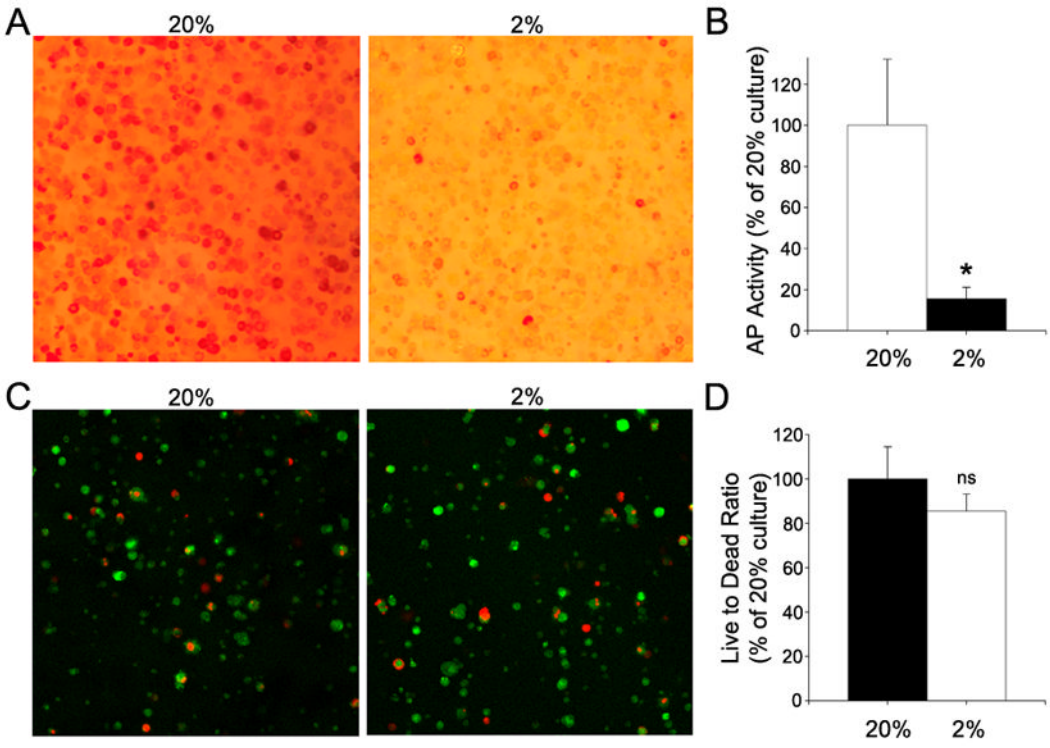

Figure 2.

Alkaline phosphate (AP) activity and viability status of by MLO-A5 cells encapsulated in alginate after 7 days culture at 20% or 2% O_2. (A) AP staining of the encapsulated cells. Note that the encapsulated cells maintained at 20% O_2 displayed robust AP staining. (B) AP activity of encapsulated MLO-A5 cells. Cells cultured at 20% O_2 exhibited higher AP activity than cells cultured at 2% O_2. AP activity is expressed as ng/min/μg total protein and normalized to 20% O_2. (C) Live/dead staining of encapsulated cells using CellTracker (green) and propidium iodide (red). Note the similarity of the staining between 2 and 20% O_2. (D) Quantification of live/dead staining. Data expressed as the ratio of CellTracker positive to propidium iodide positive cells. There was no significant difference in total cell number. Values plotted are mean and SEM. * significantly different from 20% O_2; $p<0.05$; ns non-significant.

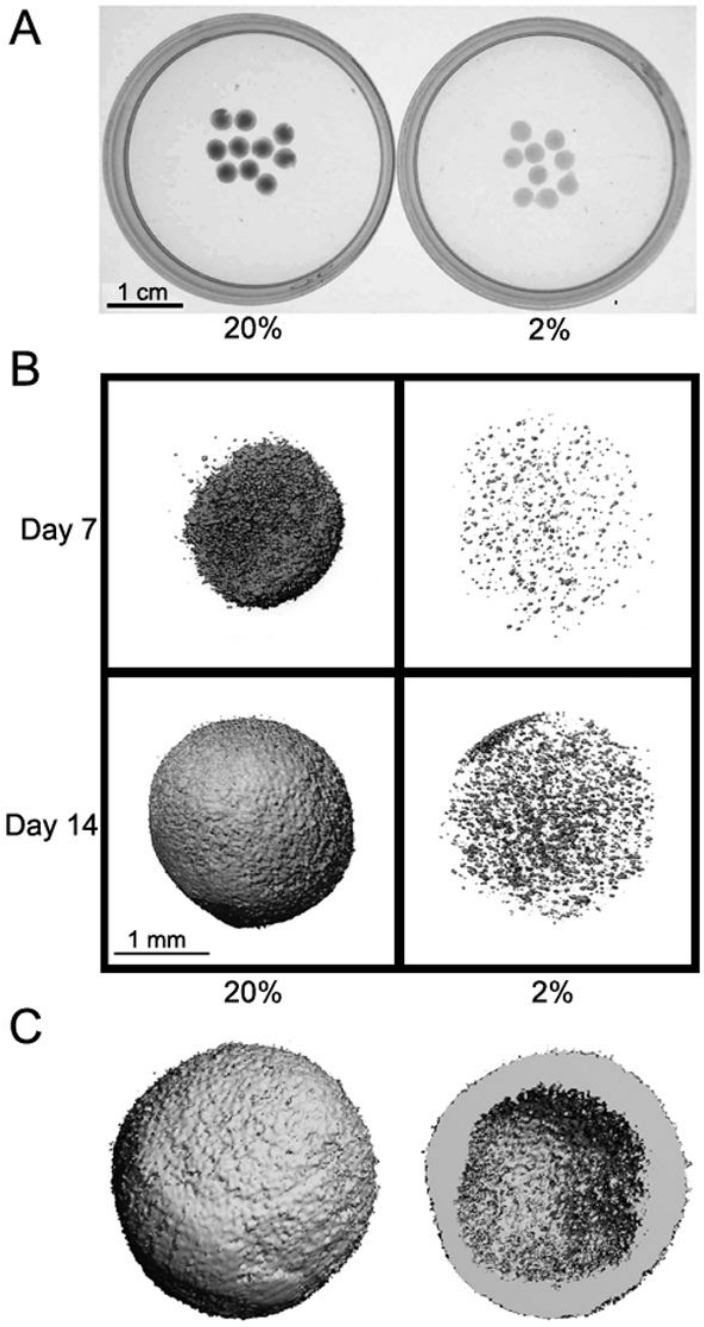

Figure 3.
Mineral deposition by encapsulated MLO-A5 cells cultured at 20 or 2% O_2. (A) Brightfield image of alginate beads after 5 days of culture. Beads were more opaque after culture in 20% O_2 than 2% O_2. (B) Computer microtomography images of alginate beads at 7 and 14 days. Note that there was greater mineral deposition at 20% than 2% O_2. (C) A cross sectional rendering of a bead cultured at 20% O_2. The image shows the deposition of a thick mineral shell.

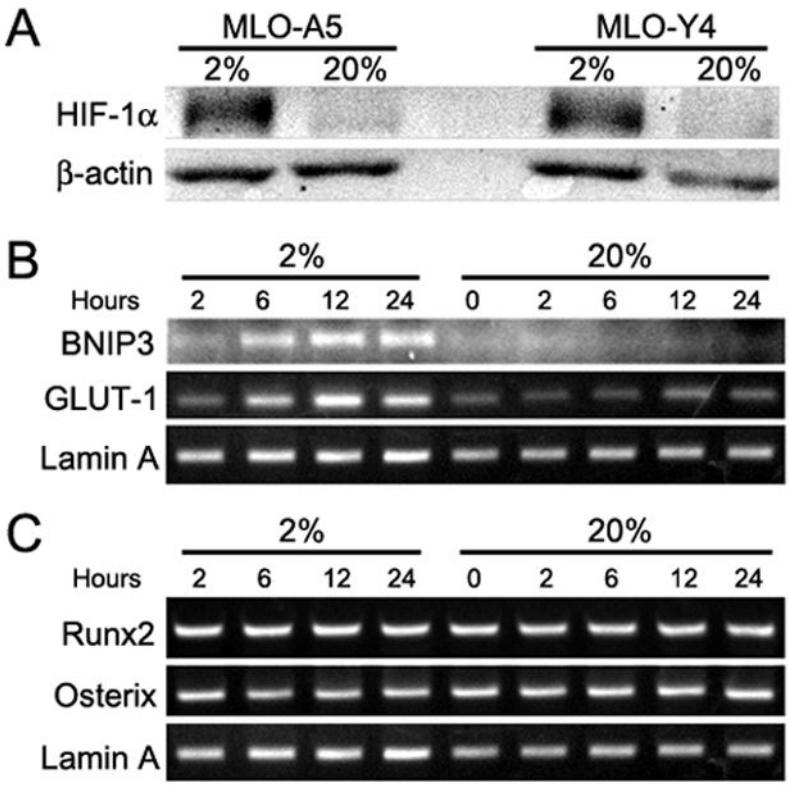

Figure 4.

Effect of O_2 concentration on the MLO-A5 phenotype. (A) Western blot analysis of HIF-1α expression by MLO-A5 and MLO-Y4 cells after culture for 24 h at 20 or 2% O_2. At 2% O_2 HIF-1α was induced in both cell types. (B) RT-PCR analysis of HIF-1α target genes expressed by MLO-A5 cells in at 20 or 2% O_2. Expression of GLUT-1 and Bnip3 was increased following culture at 2% O_2. (C) RT-PCR analysis of bone-specific transcription factors expressed by MLO-A5 cells at 20 or 2% O_2. Note that there were no changes in either RUNX2 or osterix at either O_2 concentration.

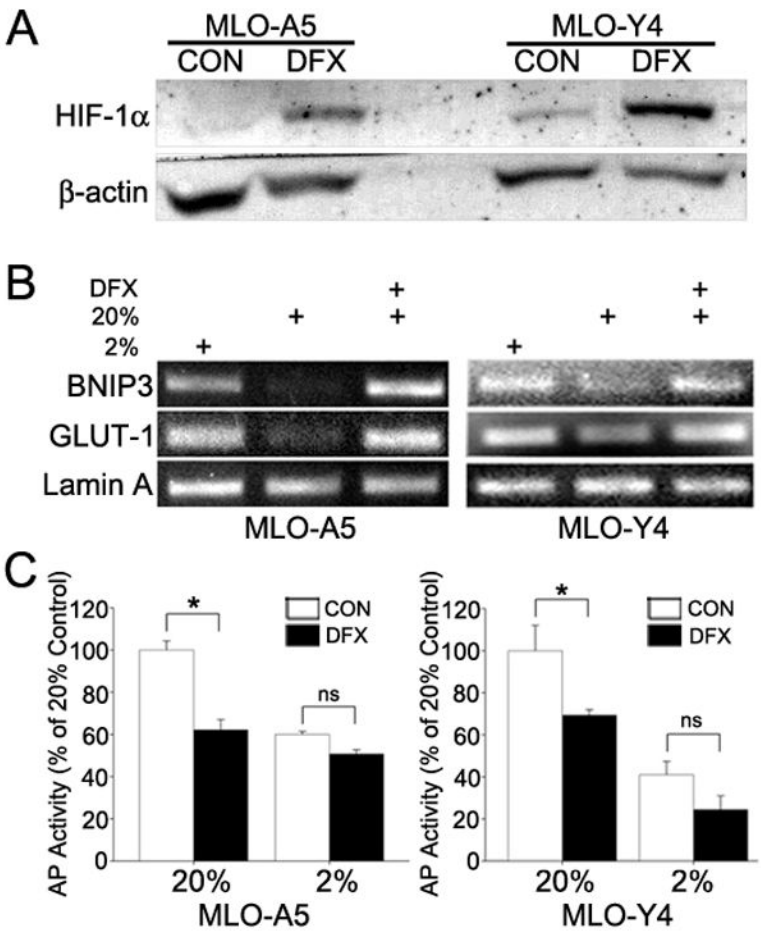

Figure 5.

HIF-1α expression, HIF-1α target gene expression and AP activity of MLO cells subjected to chemical hypoxia. (A) Western blot analysis of HIF-1α expression in MLO-A5 and MLO-Y4 cells treated with 130 m desferrioxamine (DFX) at 20% O_2 for 24 h. DFX induced HIF-1α protein expression in both cell types. (B) RT-PCR analysis of Bnip3 and GLUT1 in MLO-A5 and MLO-Y4 cells at 2% and 20% O_2, and 20% O_2 with DFX. In both cell types, the HIF-1α targets were upregulated by DFX treatment for 8 h at 20% O_2. (C) AP activity of MLO-A5 and MLO-Y4 cells treated for 24 h at 2% and 20% O_2 with or without DFX. For both cell types at 20% O_2, DFX significantly reduced AP activity. Values plotted are mean and SEM. * significantly different from untreated controls, $p<0.05$; ns denotes non-significant.

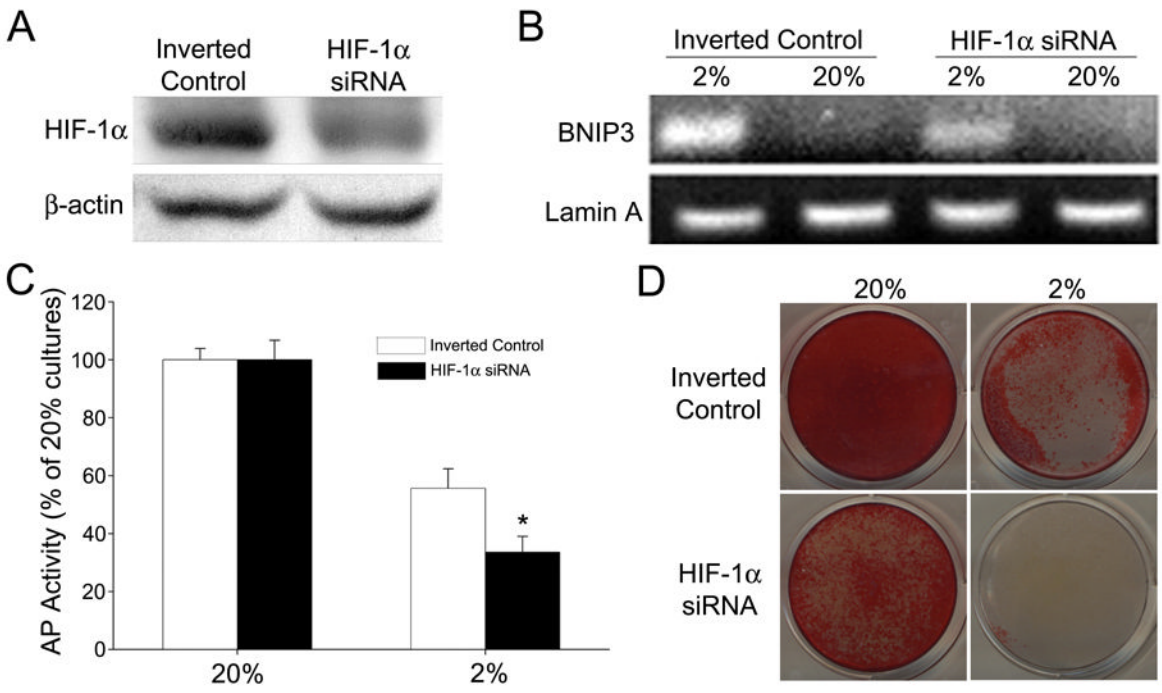

Figure 6.

Effect of HIF-1α silencing on AP activity and mineralization of MLO-A5 cells. (A) Western blot analysis of HIF-1α siRNA transfected MLO-A5 cells and cells transfected with inverted controls after 6 h at 2% O_2. HIF-1α protein expression was reduced in the silenced cells. (B) RT-PCR analysis of the HIF-1α target gene, Bnip3. There was reduced expression of Bnip3 in the silenced MLO cells maintained at 2% O_2 for 8 h. (C) AP activity of MLO-A5 cells after 7 days of culture at 20 or 2% O_2. There was a significant reduction in activity in the HIF-1α silenced cells at 2% O_2. Activity is expressed as ng/min/μg protein and normalized to 20% O_2. Values plotted are mean and SEM. * denotes significantly different from cells transfected with the inverted control at 2% pO_2; $p<0.05$. (D) Alizarin Red staining of silenced MLO-A5 cells after 7 days in culture at 20 or 2% O2. HIF-1α silenced cells displayed a reduction in staining at both O_2 tensions.

Table 1

RT-PCR primers used for detection of osteoblast gene expression

Gene	Forward Sequence (5′-3′)	Reverse Sequence (5′-3′)
Lamin A	agctagagctgagcaaagtg	gttcctcgctgtaaatgttc
Alkaline phosphatase	gctttaaacccagacacaag	gcagtaaccacagtcaaggt
Runx2	gcgtatttcagatgatgaca	taccattgggaactgatagg
Osterix	gctatctccttgcatgtctc	ggggcaataaattatcatca
BNIP3	agctccaagagttctcactg	gaaggtgctagtggaagttg
Glut-1	Tcgttggcatccttattg	gaagcttcttcagcacactc

Table 2

μCT analysis of mineral deposition by MLO-A5 cells in alginate beads

Day	O_2	MV (mm^3)	MS/MV (1/mm)
7	20%	0.397 ± 0.249	115.557 ± 38.765
	2%	0.0040 ± 0.0003	194.889 ± 3.726
14	20%	1.684 ± 0.923	38.365 ± 22.540
	2%	0.024 ± 0.003	175.267 ± 3.188

Total mineral volume (MV) and mineral surface to volume ratio (MS/MV) calculated using the plate model [31].

Values shown are mean ± SEM (n = 5).